Convolutional Perfectly Matched Layer (CPML) for the Pseudospectral Time-Domain (PSTD) Method

Juan Chen [1] and Jianguo Wang [1, 2]

[1] Key Laboratory for Physical Electronics and Devices of the Ministry of Education,
Xi'an Jiaotong University, 710049, Xi'an, China
chenjuan0306@yahoo.com.cn

[2] Northwest Institute of Nuclear Technology; P. O. Box 69-15, Xi'an 710024, China

Abstract ─ In this paper, a perfectly matched layer (PML) medium with complex frequency shifted (CFS) constitutive parameters is introduced into the two-dimensional pseudospectral time-domain (PSTD) algorithm. The absorbing performance and computational efficiency of the method are illustrated by comparing with the PML method. It shows that no matter what spatial discretization is used, the reflection relative error of convolutional perfectly matched layer (CPML) is almost the same as that of the PML method. The total flops counts of the PSTD-CPML method are reduced from 49 to 34 compared with that of the PSTD-PML method. This corresponds to an efficiency gain of 1.44 in flops count reduction for the PSTD-CPML method.

Index Terms - Convolutional perfectly matched layer (CPML) and pseudospectral time-domain (PSTD) algorithm.

I. INTRODUCTION

Recently, the pseudospectral time-domain (PSTD) method has been introduced for solving Maxwell's equation [1-5]. In this method, the spatial discretization only needs two cells per wavelength. This method is extremely useful for problems with electrically large structure. For solving these problems the PSTD method is more efficient than the finite-difference time-domain method (FDTD) method in terms of computer memory. Due to the important impact of PSTD method on the electromagnetic computation, an accurate and efficient absorbing boundary condition must be developed to simulate electromagnetic interaction in an unbounded space.

In the initial implementation of the PSTD method in [1, 2], a split-step perfectly matched layer (PML) is used due to its broad band absorption characteristics and application to general media. Nevertheless, a split-field PML based on Berenger's original formulation [5-7] needed to split the field components and the implementation is complex compared with the original PSTD method.

Roden *et al.* [8] have demonstrated that the complex frequency shifted (CFS) constitutive PML parameters originally introduced by Kuzuoglu and Mittra [9] result in a PML that is highly effective at absorbing low-frequency evanescent waves. Their implementation, referred to as the convolutional-PML (CPML) method, allows the PML medium to be placed directly in the near field of geometric aberrations and can accurately absorb low-frequency waves.

In this paper, the CPML technique is introduced into the PSTD method. It is not needed to split the field components. The effectiveness of the method is illustrated through numerical examples. It is demonstrated that the reflection relative error of the CPML can reach to -70 dB, which shows good absorbing performance of the CPML method. Besides, compared with the PSTD-PML method, the PSTD-CPML method can reduce the total flops counts from 49 to 34. This corresponds to a gain of 1.44 in the computation time reduction for the PSTD-CPML method.

Submitted On: Nov. 21, 2012
Accepted On: May 13, 2013

II. FORMULATIONS

The formulations of PSTD method inclusion of CPML are presented in equations (1) to (3),

$$H_y^{n+1/2}(m,p) = H_y^{n-1/2}(m,p) + \frac{\Delta t}{\mu}\left[\frac{\partial E_z^n(m,p)}{k_x(m)\partial x} + \Phi_{Hyx}^n(m,p)\right] \quad (1)$$

$$H_x^{n+1/2}(m,p) = H_x^{n-1/2}(m,p) - \frac{\Delta t}{\mu}\left[\frac{\partial E_z^n(m,p)}{k_y(p)\partial y} - \Phi_{Hxy}^n(m,p)\right], \quad (2)$$

$$E_z^{n+1}(m,p) = E_z^n(m,p) + \frac{\Delta t}{\varepsilon}\left[\begin{array}{l}\dfrac{\partial H_y^{n+1/2}(m,p)}{k_x(m)\partial x} - \dfrac{\partial H_x^{n+1/2}(m,p)}{k_y(p)\partial y} \\ +\Phi_{Ezx}^{n+1/2}(m,p) - \Phi_{Ezy}^{n+1/2}(m,p)\end{array}\right]. \quad (3)$$

Convolutional perfectly matched layer is introduced by the variables Φ and k_s. The symbol k_s is the spatially scaled in the PML layer. Its expression is,

$$k_s(s) = 1 + (k_{\max} - 1)\frac{|s - s_0|^r}{d^r} \qquad s = x, y \quad (4)$$

where s_0 is the CPML interface, d is the depth of the CPML, r is the order of the polynomial, $k_{\max}$ is the maximum values of k_s at the exterior boundary. The expressions of Φ are as follows,

$$\Phi_{Hyx}^{n+1}(m,p) = b_x(m)\Phi_{Hyx}^n(m,p) + a_x(m)\frac{\partial E_z^{n+1}(m,p)}{\partial x} \quad (5)$$

$$\Phi_{Hxy}^{n+1}(m,p) = b_y(p)\Phi_{Hxy}^n(m,p) + a_y(p)\frac{\partial E_z^{n+1}(m,p)}{\partial y}, \quad (6)$$

$$\Phi_{Ezx}^{n+1/2}(m,p) = b_x(m)\Phi_{Ezx}^{n-1/2}(m,p) + a_x(m)\frac{\partial H_y^{n+1/2}(m,p)}{\partial x}, \quad (7)$$

$$\Phi_{Ezy}^{n+1/2}(m,p) = b_y(p)\Phi_{Ezy}^{n-1/2}(m,p) + a_y(p)\frac{\partial H_x^{n+1/2}(m,p)}{\partial y}, \quad (8)$$

where

$$b_s(s) = e^{-\left((\sigma_s(s)/k_s(s)) + \alpha_s\right)(\Delta t/\varepsilon_0)}$$

$$a_s(s) = \frac{\sigma_s(s)}{k_s(s)\left(\sigma_s(s) + k_s(s)\alpha_s\right)}\left(b_s(s) - 1\right).$$

The symbol σ_s are the conductivity in the PML. Within the host medium, the values of k_s are equal to 1, and all the variables Φ become zeros, then equations (1) to (3) are the standard formulations of the PSTD method [1].

The spatial derivatives in equations (1) to (7) should be replaced with the PS scheme, for example,

$$\begin{aligned}\frac{\partial E_z^n(x,y)}{\partial x}\Big|_{x=m\Delta x, y=p\Delta y} &= FFT_x^{-1}\left\{jk_x FFT_x\left[E_z^n(x, p\Delta y)\right]\right\}\Big|_{x=m\Delta x} \\ &= \frac{1}{2\pi}\sum_{l=0}^{M-1} jk_{x,l}\tilde{E}_z^n(k_{x,l}, p\Delta y)e^{jk_{x,l}(m\Delta x)}\Delta k_x\end{aligned} \quad (9)$$

where FFT and FFT^{-1} stand for the fast Fourier transform and its inverse transform. $\tilde{E}_z^n(k_{x,l}, p\Delta y) = \sum_{m=0}^{M-1} E_z^n(m\Delta x, p\Delta y)e^{-jk_{x,l}(m\Delta x)}\Delta x$ is the Fourier transforms of $E_z^n(x, p\Delta y)$. The symbol j is a complex symbol. Δx and Δy are the spatial increments in x and y directions; m and p denote the indices of the spatial increments; M is the total mesh cell in the x direction. The range of spectral domain k_x is in the form of $-2\pi/2\Delta x$ to $2\pi/2\Delta x$, so, $k_{x,l} = -\frac{2\pi}{2\Delta x} + l\Delta k_x$, $\Delta k_x = \frac{2\pi}{M\Delta x}$.

Unlike the previous PSTD-PML formula [1, 2], the PSTD-CPML formula is not needed to split the field components and the implementation is convenient.

III. THE COMPUTATIONAL EFFICIENCY OF THE CPML-PSTD COMPARED WITH PML-PSTD

To compare the computational efficiency of the PSTD-CPML method with that of the PSTD-PML method, we recall the updating equation of the PSTD-PML method as follows,

$$H_y^{n+1/2}(m,p) = \exp(-\sigma_{my}(p)\Delta t/\mu_0) H_y^{n-1/2}(m,p) + \frac{1-\exp(-\sigma_{my}(p)\Delta t/\mu_0)}{\sigma_{my}(p)} FFT^{-1}\left[jk_x \tilde{E}_z^n(m,p)\right] \tag{10}$$

$$H_x^{n+1/2}(m,p) = \exp(-\sigma_{mx}(m)\Delta t/\mu_0) H_x^{n-1/2}(m,p) - \frac{1-\exp(-\sigma_{mx}(m)\Delta t/\mu_0)}{\sigma_{mx}(m)} FFT^{-1}\left[jk_y \tilde{E}_z^n(m,p)\right], \tag{11}$$

$$E_{zx}^{n+1}(m,p) = \exp(-\sigma_x(m)\Delta t/\varepsilon_0) E_{zx}^n(m,p) + \frac{1-\exp(-\sigma_x(m)\Delta t/\varepsilon_0)}{\sigma_x(m)} FFT^{-1}\left[jk_x \tilde{H}_y^{n+1/2}(m,p)\right], \tag{12}$$

$$E_{zy}^{n+1}(m,p) = \exp(-\sigma_y(p)\Delta t/\varepsilon_0) E_{zy}^n(m,p) - \frac{1-\exp(-\sigma_y(p)\Delta t/\varepsilon_0)}{\sigma_y(p)} FFT^{-1}\left[jk_y \tilde{H}_x^{n+1/2}(m,p)\right], \tag{13}$$

$$E_z^{n+1}(m,p) = E_{zx}^{n+1}(m,p) + E_{zy}^{n+1}(m,p). \tag{14}$$

The floating point operations (flops) counts taking into account the number of multiplications /divisions (M/D), additions/subtractions (A/S), exponentiation and Fourier transform (FT) required for one complete time step for PSTD-CPML and PSTD-PML methods are listed in Table I, based on the right-hand sides of their respective updating equations. For simplicity, the number of electric and magnetic field components in all directions has been taken to be the same and assume that all multiplicative factors have been pre-computed and stored. From the table, it is clear that the total flops counts for the PSTD-CPML method are reduced from 49 to 34 compared with that of the PSTD-PML method. This corresponds to an efficiency gain of 1.44 in flops count reduction for the PSTD-CPML method.

Table I: Flops count for PSTD-CPML and PSTD-PML algorithms.

	A/S	M/D	FT	exponentiation
PSTD-CPML	12	18	4	0
PSTD-PML	9	28	4	8

IV. NUMERICAL RESULTS

To illustrate the CPML termination of the PSTD lattice, a simulation of a small current source radiating in free space is studied. A uniform mesh with cell spacing $\Delta x = \Delta y = 0.01$ *m* and lattice dimension of 200 × 200 is considered. The reflection error due to the CPML is studied by exciting a small current source at the center of the grid. The time dependence of the source is,

$$g(t) = \exp\left[\frac{-4\pi(t-t_0)^2}{t_1^2}\right] \tag{15}$$

where t_0 and t_1 are constants, and both equal to 1×10^{-9}. The highest frequency of the Gauss source is determined by the value $2/t_1$ = 2 GHz, thus the minimum wavelength of the source is about 0.15 *m*. The spatial discretization Δx is equal to 1/15 of the minimum wavelength. The reflection error is computed at the source point. A reference solution based on an extended lattice is computed in order to isolate the error due to the CPML from grid dispersion error. The relative error is computed as,

$$err(\mathrm{dB}) = 20\log_{10}\frac{\left|E(t)-E^{std}(t)\right|}{\left|E^{std}(t)\right|} \tag{16}$$

where $E^{std}(t)$ is the value of the electric field at that point computed by the extended lattice PSTD. $E(t)$ is the electric field calculated by the PSTD truncated by the CPML.

CPML layers that are twenty cells thick terminate all four sides of the lattice. Within the CPML, the conductivity is selected as,

$$\sigma_s(s) = \frac{\sigma_{s\max}\left|s-s_0\right|^r}{d^r}\ . \tag{17}$$

A choice for $\sigma_{s\max}$ that will minimize the reflection is expressed as,

$$\sigma_{s\max} = \frac{(r+1)}{150\pi\Delta s} \tag{18}$$

where Δs is the grid spacing along the normal axis. The time step is selected as $\Delta t = 2\Big/\pi c\sqrt{(1/\Delta x)^2+(1/\Delta y)^2}$ = 15 ps, which is

the maximum time step to satisfy time stability condition in the PSTD method, where c is the speed of light within the host medium. The reflection error with respect to time step is showed in Fig. 1. For the sake of comparison, the reflection error of the PSTD-PML method is also plotted in this figure. As can be seen from this figure, both the reflection relative error of CPML and PML are less than -70 dB. It means that the CPML has almost the same absorbing performance as the PML method.

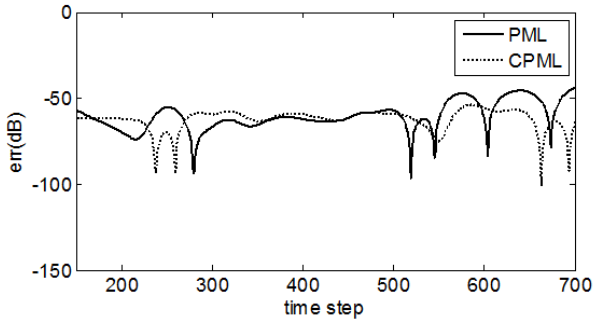

Fig. 1. The reflection relative error of CPML and PML with Δt = 15 ps.

The significant feature of the PSTD method is its spatial discretization, which only needs two cells per wavelength. So, we can increase the spatial increments of the PSTD method to $\Delta x = \Delta y$ = 0.075 m, corresponding to 1/2 of the wavelength. The reflection error with this spatial increment is plotted in Fig. 2. The time step size is selected as the maximum to satisfy the limitation of the stable condition in the PSTD method. It is $\Delta t = 2/\pi c\sqrt{(1/\Delta x)^2 + (1/\Delta y)^2}$ = 112.5 ps, which is seven times as that of the conventional FDTD method. It can be seen from Fig. 2 that the reflection relative error of the CPML method is also the same as that of the PML method, but due to very large time step size and spatial discretization used, both the reflection relative error of the CPML and PML become a little larger than the results in Fig. 1, especially in the late response. The reflection relative error reach to -50 dB after 400 time steps. However, it does not affect the application of the CPML method in the situation not with very stringent absorbing performance requirements.

It should be noted that when spatial increments of the PSTD method increase to 1/2 wavelength, some ripples appears in the reflection relative error of the CPML method, as shown in Fig. 2. This is duo to the wraparound effect of the PSTD method, which can be eliminated by using PML cells at the outer boundary.

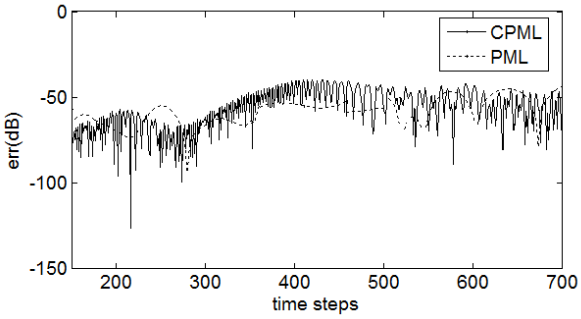

Fig. 2. The reflection relative error of the CPML with Δt = 112.5 ps.

One advantages of the CPML lies in its capability of dealing with the low frequency evanescent waves. Therefore, it is necessary to show the reflection relative error in the simulated frequency domain. The variation of the reflection relative error of the PSTD-CPML method with respect to frequency is plotted in Fig. 3. It can be seen from this figure that in the entire frequency range (including the low frequency band) the reflection relative error of CPML is less than -50 dB and it is highly effective at absorbing low-frequency evanescent waves. The CPML parameters r and $k_{\max}$ are selected by using the method in references [10] and [11].

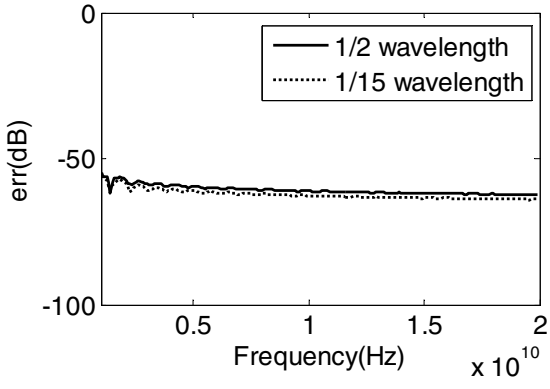

Fig. 3. Variation of the reflection relative error of the PSTD-CPML method with respect to frequency.

V. CONCLUSION

A pseudospectral time-domain method employing the CPML equations is presented. It is not needed to split the field components. Numerical example demonstrates that the reflection relative error of CPML is less than -70 dB and shows good absorbing performance of the convolutional perfectly matched layer.

ACKNOWLEDGMENT

This work was supported by the National Natural Science Foundations of China (No. 61001039 and 61231003), and also supported by the Fundamental Research Funds for the Central Universities.

REFERENCES

[1] Q. H. Liu, "The PSTD algorithm: A time-domain method requiring only two cells per wavelength," *Microwave Opt. Technol. Lett.*, vol. 15, pp. 158-165, 1997.

[2] Q. Li and Y. Chen, "Application of the PSTD for scattering analysis," *IEEE Trans. Antennas Propagat.*, vol. 50, pp. 1317-1319, 2002.

[3] Q. H. Liu and G. Fan, "A frequency-dependent PSTD algorithm for general dispersive media," *IEEE Microwave Guided Wave Lett.*, vol. 9, pp. 51-53, 1999.

[4] Z. Lin, Y. Jia, P. Ou, and C. Zhang, "A Full-spectrum numerical-dispersion compensation Technique for the Pseudospectral time-domain method," *IEEE Antennas and Wireless Propagation Lett.*, vol. 11, pp. 212-215, 2012.

[5] J. P. Berenger, "A perfectly matched layer for the absorption of electromagnetic waves," *J. Comput. Phys.*, vol. 114, pp. 185-200, 1994.

[6] J. P. Berenger, "Improved PML for the FDTD solution of wave-structure interaction problems," *IEEE Trans. Antennas Propagat.*, vol. 45, pp. 466-473, 1997.

[7] J. P. Berenger, "An effective PML for the absorption of evanescent waves in waveguides," *IEEE Microwave Guided Wave Lett.*, vol. 8, pp. 188-190, 1998.

[8] J. A. Roden and S. D. Gedney, "Convolutional PML (CPML): An efficient FDTD implementation of the CFS-PML for arbitrary media," *Microwave Opt. Technol. Lett.*, vol. 27, pp. 334-339, 2000.

[9] M. Kuzuoglu and R. Mittra, "Frequency dependence of the constitutive parameters of causal perfectly matched anisotropic absorbers," *IEEE Microwave Guided Wave Lett.*, vol. 6, pp. 447-449, 1996.

[10] J. P. Bérenger, "Application of the CFS PML to the absorption of evanescent waves in waveguides," *IEEE Microwave and Wireless Components Lett.*, vol. 12, pp. 218-220, 2002.

[11] M. F. Hadi, "Near-field PML optimization for low and high order FDTD algorithms using closed-form predictive equations," *IEEE Trans. Antennas Propagat.*, vol. 59, pp. 2933-2941, 2011.